Available online at www.sciencedirect.com
ScienceDirect
Nuclear Physics B Proceedings Supplement 00 (2012) 1–4
Nuclear Physics B Proceedings Supplement

J/ψ, $\Upsilon(1S)$ and $\chi_b(3p)$ Production Measurement with the ATLAS Detector

Rui Wang

Department of Physics and Astronomy, University of New Mexico
Albuquerque, NM, USA, 87131

On behalf of the ATLAS Collaboration.

Abstract

The J/ψ and $\Upsilon(1S)$ production cross-sections are measured in proton-proton collisions using the ATLAS detector at the LHC. Differential cross-sections are measured as a function of transverse momentum and rapidity. Results are compared to QCD predictions. A new χ_b state has been observed though radiative transitions to the $\Upsilon(1S)$ and $\Upsilon(2S)$ states.

Keywords: production cross-section, differential cross-section, J/ψ, $\Upsilon(1S)$, χ_b, LHC, ATLAS experiment
2000 MSC: 074220

1. Introduction

The production of heavy quarkonium at hadron colliders provides particular challenges and opportunities for insight into the theory of Quantum Chromodynamics (QCD) as its mechanisms of production operate at the boundary of the perturbative and non-perturbative regimes. Despite being among the most studied of the bound-quark systems, there is still no clear understanding of the mechanisms in the production of quarkonium states like the J/ψ and Υ that can consistently explain both the production cross-section and spin-alignment measurements. Data obtained by the Large Hadron Collider (LHC) can help to test existing theoretical models of both quarkonium production and b-production in a new energy regime.

Indent the most important elements of the ATLAS detector for B-physics measurements are the Inner Detector (ID) tracker and the Muon Spectrometer, details can be found in [1]. Dedicated B physics triggers are based on both single muons and di-muons with different thresholds and mass ranges.

2. Measurement of the differential cross-sections for inclusive, prompt and non-prompt J/ψ production

The inclusive J/ψ production cross-section is measured in the $J/\psi \to \mu^+\mu^-$ decay channel as a function of both J/ψ transverse momentum and rapidity using 2.3 pb^{-1} of ATLAS 2010 7 TeV data [2]. Data are collected via a single muon trigger, with a threshold that grows from 4 GeV to 6 GeV as the instantaneous luminosity increases. The J/ψ yields are determined by the number of J/ψ candidates which are extracted from the observed di-muon pairs, with weights applied to unfold the acceptance, detector resolution, tracking, reconstruction and trigger efficiencies in each p_T and rapidity bin. Because the spin alignment of the J/ψ is unknown at the LHC, an envelope of all possible spin alignment assumptions is taken and assigned as an additional systematic uncertainty.

Figure 1 shows the measurement of the differential cross-sections of inclusive J/ψ production, with the CMS result [3] included for comparison. The ATLAS

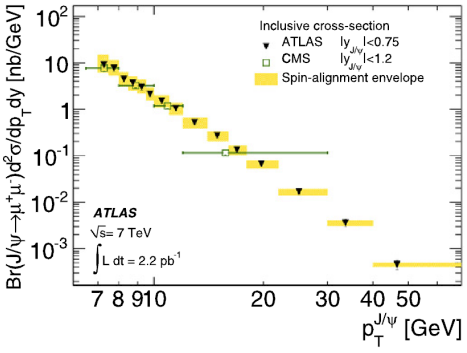

Figure 1: The inclusive J/ψ production cross-section as a function of J/ψ transverse momentum in the $|y| < 0.75$ rapidity bin. The CMS result is included for comparison.

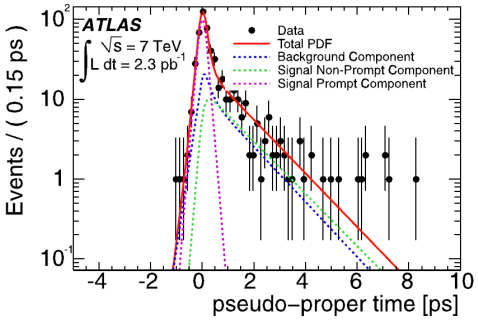

Figure 2: Pseudo-proper time distributions (top) of $J/\psi \to \mu^+\mu^-$ candidates in the signal region, for example bin $9.5 < p_T < 10.0$ GeV and $|y| < 0.75$ regions. The points with error bars are data. The solid line is the result of the maximum likelihood unbinned fit to all di-muon pairs in the 2.5 - 3.5 GeV mass region projected on the narrow mass window 2.9 - 3.3 GeV.

and CMS results agree well in the overlapped regime.

It is possible to distinguished the prompt J/ψ's produced directly from the p-p collision from the non-prompt J/ψ's produced in B-hadron decays by the measurably displaced decay point due to the long lifetime of their B-hadron parent. A simultaneous unbinned maximum likelihood fit is applied to both invariant mass and lifetime (Figure 2), which allows us to determine the fraction of non-prompt J/ψ as a function of p_T and rapidity. The result for one of the rapidity slices is shown in Figure 3, in good agreement with the CMS result [3]. This fraction is strongly dependent on $p_T^{J/\psi}$ with only weak dependence on $\eta^{J/\psi}$. The result has been compared to CDF result [4] indicating a limited dependence on collision energy.

By combining the results of the inclusive J/ψ cross-section and non-prompt J/ψ fraction in each p_T and rapidity bin, the non-prompt and prompt J/ψ differential cross-section can be extracted. The non-prompt J/ψ

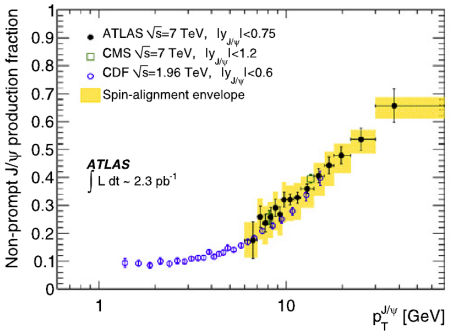

Figure 3: The non-prompt J/ψ to inclusive fraction as a function of J/ψ transverse momentum. Overlaid is a band representing the variation of the result under various spin-alignment scenarios. The equivalent results from CMS and CDF are included.

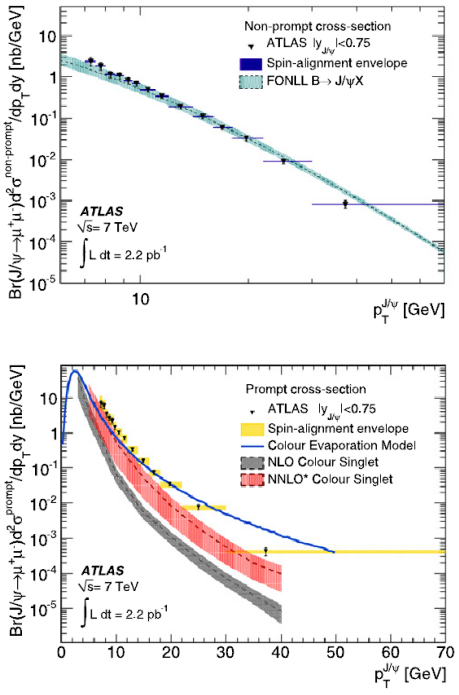

Figure 4: Non-prompt (top) and prompt (bottom) J/ψ production cross-sections as a function of J/ψ transverse momentum with $|y| < 0.75$. Non-prompt results are compared to FONLL predictions. Prompt results are compared to NLO and NNLO and Colour Evaporation Model predictions. Overlaid is a band representing the variation of the result under various spin-alignment assumptions on the non-prompt and prompt components. The central value assumes an isotropic polarization for both prompt and non-prompt production.

results are in a good agreement with the Fixed Order Next-to-Leading-Log (FONLL) prediction [5][6]. The prompt J/ψ results are compared to the Colour Evaporation Model (CEM) [7] and Colour Singlet Model(CSM) [8][9]. The Colour Evaporation Model showing significant disagreement in the extended p_T range. The Colour Singlet Model with an NNLO calculation shows significant improvement in describing the p_T dependence and normalization of prompt J/ψ production over the NLO calculation but is still lower than the data. This is expected to be relatively significant for hidden charm production. Result in the regime $|y| < 0.75$ is shown in Figure 4.

3. Measurement of the $\Upsilon(1S)$ production cross-section

The $\Upsilon(1S)$ production cross-section is measured in the $\Upsilon(1S) \rightarrow \mu^+\mu^-$ decay channel as a function of both $\Upsilon(1S)$ transverse momentum and rapidity using 1.13 pb^{-1} of ATLAS 2010 7 TeV data [12]. Muons are selected via a single muon trigger with a threshold of 4 GeV and are required to have $p_T > 4$ GeV and $|\eta| < 2.5$ in order to remove the uncertainty associated with spin alignment in the cross-section measurement. The $\Upsilon(1S)$ yields are determined by correcting the number of reconstructed $\Upsilon(1S)$ candidates with weights which unfold the trigger and reconstruction efficiencies in each p_T and rapidity bin.
Indent the results are compared to both NLO and NRQCD predictions (Figure 5). The data significantly exceed the NLO prediction but this may be explained by contributions from higher mass bound states and by the need for additional higher order corrections to $\Upsilon(1S)$ production. In contrast, the data are in reasonable agreement with the NRQCD prediction as implemented in Pythia8 but differences in the shape of the p_T spectrum of about a factor of two are observed.

4. Observation of a new χ_b state in radiative transitions to $\Upsilon(1S)$ and $\Upsilon(2S)$

The $\chi_b(nP)$ quarkonium states are studied using a data sample corresponding to an integrated luminosity of 4.4 fb^{-1} of ATLAS 2011 data [13]. Previous experiments have measured the $\chi_b(1P)$ and $\chi_b(2P)$ through decay modes of $\chi_b(nP) \rightarrow \Upsilon(1S)\gamma$ and $\chi_b(nP) \rightarrow \Upsilon(2S)\gamma$.
Indent $\Upsilon(1S) \rightarrow \mu\mu$ candidates with masses in the

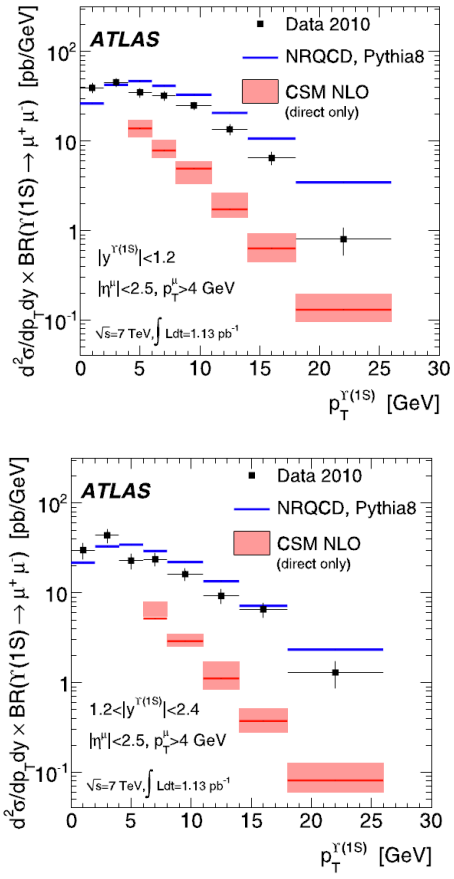

Figure 5: The differential $\Upsilon(1S)$ cross-section for $|y^{\Upsilon(1S)}| < 1.2$ (top) and $1.2 < |y^{\Upsilon(1S)}| < 2.4$ (bottom) as a function of $p_T^{\Upsilon(1S)}$ for $p_T^{\mu} > 4$ GeV and $|\eta| < 2.5$ on both muons. Also shown is the colour-singlet NLO (CSM) [10] prediction using $m_T = \sqrt{4m_b^2 + p_T^2}$ ($m_b = 4.75$ GeV) for the renormalisation and factorization scales. The shaded area shows the change in the theoretical prediction when varying the renormalisation and factorization scales by a factor of two. The CSM NLO calculation accounts only for direct production of $\Upsilon(1S)$ mesons and not for any feed-down from excited states. The NRQCD prediction as implemented in Pythia8 [11] is also shown for a particular choice of parameters.

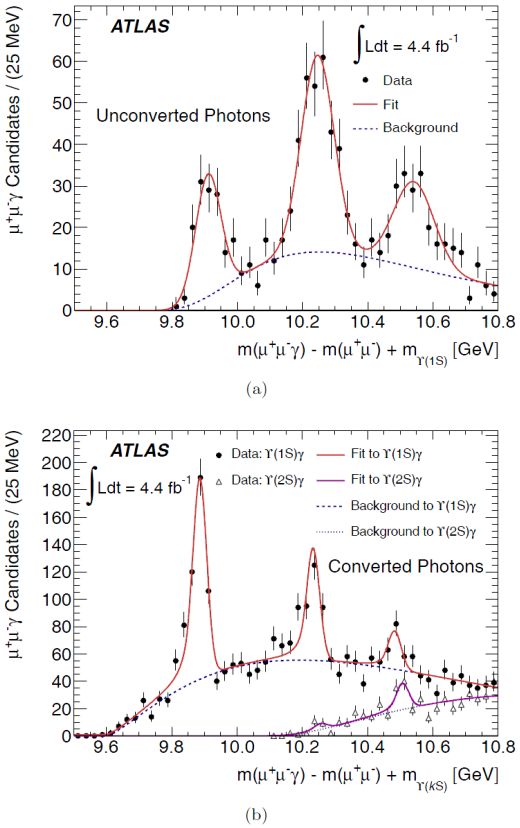

Figure 6: (a) The mass distribution of $\chi_b \to \Upsilon(1S)\gamma$ candidates for unconverted photons reconstructed from energy deposits in the electromagnetic calorimeter. (b) The mass distributions of $\chi_b \to \Upsilon(kS)\gamma$ (k = 1, 2) candidates formed using photons which have converted and been reconstructed in the ID. Data are shown before the correction for the energy loss from the photon conversion electrons due to bremsstrahlung and other processes. The data for decays of $\chi_b \to \Upsilon(1S)\gamma$ and $\chi_b \to \Upsilon(2S)\gamma$ are plotted using circles and triangles respectively. Solid lines represent the total fit result for each mass window. The dashed lines represent the background components only.

ranges $9.25 < m_{\mu\mu} < 9.65$ GeV and $\Upsilon(2S) \to \mu\mu$ candidates with masses in the ranges $9.80 < m_{\mu\mu} < 10.10$ GeV are selected. A photon is combined with each. Photons are reconstructed by using ID tracks from e^+e^- pairs with a conversion vertex or electromagnetic calorimeter energy deposit. As shown in the mass difference $m(\mu^+\mu^-) - m(\mu^+\mu^-\gamma)$ distributions (Figure 6), in addition to the mass peaks corresponding to the decay modes $\chi_b(1P, 2P) \to \Upsilon(1S)$, a new structure centered at mass $10.530 \pm 0.005(stat.) \pm 0.009(syst.)$ GeV is also observed. This is interpreted as the $\chi_b(3P)$ state.

References

[1] ATLAS Collaboration, JINST **3** (2008) S08003.
[2] ATLAS Collaboration, Physics Letters B **850** (2011) 387 – 444.
[3] CMS Collaboration, V. Khachatryan, et al., CMS-BPH-10-002, CERN-PH-EP-2010-046, arXiv:1011.4193 [hep-ex].
[4] CDF Collaboration, T. Aaltonen, et al. , Phys. Rev. D **71** (2005) 032001.
[5] P. N. M. Cacciari, M. Greco, JHEP **9805** (1998) 007.
[6] P. N. M. Cacciari, M. Greco, JHEP **0103** (2001) 006.
[7] R. V. T. Ullrich, A.D. Frawley, Phys. Rep. **462** (2008) 125.
[8] J. L. S.J. Brodsky, Phys. Rev. D **81** (2010) 051502(R).
[9] J. Lansberg, Eur. Phys. J. C **61** (2009) 693.
[10] F. T. J. Campbell, F. Maltoni, Phys. Rev. Lett. **98** (2007) 252002.
[11] PYTHIA version 8.135, T. Sjostrand, S. Mrenna, P. Skands, Comput. Phys.Comm. **178** (2008) 852.
[12] ATLAS Collaboration, Physics Letters B **705** (2011) 9 – 27.
[13] ATLAS Collaboration, Phys. Rev. Lett. **108** (2012) 152001.